Asian Journal of Advanced Research and Reports

Volume 18, Issue 11, Page 216-224, 2024; Article no.AJARR.118040
ISSN: 2582-3248

Inter-Connection between Refractivity Gradient Variations and Intertropical Discontinuity over Nigeria

Ogodo S.O [a*] and Abosede S.A [a]

[a] Federal College of Agriculture, Akure, Nigeria.

Authors' contributions

This work was carried out in collaboration between both authors. Both authors read and approved the final manuscript.

Article Information

DOI: https://doi.org/10.9734/ajarr/2024/v18i11789

Open Peer Review History:
This journal follows the Advanced Open Peer Review policy. Identity of the Reviewers, Editor(s) and additional Reviewers, peer review comments, different versions of the manuscript, comments of the editors, etc are available here: https://www.sdiarticle5.com/review-history/118040

Original Research Article

Received: 15/04/2024
Accepted: 18/06/2024
Published: 04/11/2024

ABSTRACT

Radio signal transmission is significantly impacted by the troposphere's complexity. As a result, refractivity gradients has been a crucial parameter for path clearance estimation and propagation effects including ducting, super-refraction, and sub-refraction. Through empirical formulations, this study focuses on the correlations that exist between Intertropical Discontinuity (ITD) and Refractivity Gradient. One important factor influencing West African weather patterns is the ITD. Utilising hourly temperature and relative humidity data for the years 2017 and 2018 at two levels (surface and 1000 hpa) gathered from the archives of the European Centre for Medium-Range Forecasts (ECMWF) for twenty meteorological stations in Nigeria, the refractivity gradient values were computed. Using ANOVA method, five regression models (Linear, Cubic, Quadratic, Power and Log) were developed between refractivity gradient and ITD. The linear model ($L = B_0 + B_1RG$) have been found to be mostly significant with coefficient of determination ranging between 97% and 99%) across all the regions.

**Corresponding author: Email: ogodosegun@gmail.com;*

Cite as: *S.O, Ogodo, and Abosede S.A. 2024. "Inter-Connection Between Refractivity Gradient Variations and Intertropical Discontinuity over Nigeria". Asian Journal of Advanced Research and Reports 18 (11):216-24. https://doi.org/10.9734/ajarr/2024/v18i11789.*

Keywords: Radio signal transmission; meteorological stations; refractivity gradient; radiation.

1. INTRODUCTION

The temperature and humidity variations in Nigeria cause the intertropical discontinuity, which considerably aids in the formation of the refractivity gradient [1, 2, 3]. Using radiosonde recordings, [4] conducted study on the refractivity gradient along the Intertropical discontinuity. The large temperature and moisture content variations among the various trade wind systems lead the area to suffer a refractivity gradient, which is mostly governed by the intertropical discontinuity zone [5, 6, 7, 8, 9, 10, 11].

Horizontal layers with highly variable refractivity greatly show the large-scale variations in the refractive index of the atmosphere [12,13]. Multipath effects are produced when there are significant variations in the refractive index due to large-scale variations in the atmospheric radio refraction index [14,15]. The condition is especially true if the same signal reaches its objective and then battles with another signal along the way, reaching a lapse in the troposphere that attends it [16, 17]. The large-scale difference in refractive index provides an explanation; radiation passing through the atmosphere gently bends as it moves across the earth [18, 19]. Thus, the altitude dependence of the refractivity determines the radio wave's reach. Consequently, the path's curve will be influenced by the atmosphere's refractivity [3, 20]

Radar systems that are active in the tropics are likewise impacted by the intertropical discontinuity's effect on the refractivity gradient [21, 19, 22] conducted research to investigate the influence that the ITD has on the performance of weather radar. They discovered that the fluctuations in the refractivity gradient that occur over the ITD might cause errors to be introduced into radar data, which in turn affects how accurately rainfall estimation and storm tracking are performed [23, 24, 25].

2. METHODOLOGY

2.1 Site Description

The study was carried out on 19 locations in Nigeria, namely: Sokoto, Kastina, Kano, Maiduguri, Ibadan, Ado-Ekiti, Ogbomosho, Ilorin, Osogbo, Lagos, Yenagoa, Benin, Port Harcourt, Warri, Minna, Jos, Abeokuta, Bida and Abuja; whose geographical coordinate are presented. The terrain is divided into four distinct regions: the Coastal, Derived Savannah, Guinea and Sub-Sahelian Region. Regarding the many kinds of tropical climates, the position of the Intertropical Discontinuity is the factor that has the most significant influence on the climate. The ITD is a low-pressure region that denotes the place where the trade winds converge. The position of the ITD shifts during the course of the year, and although it stays relatively close to the equator, the ITD over land tends to move to latitudes that are farther north or south than the ITD over sea. This is because of the wider range in temperature throughout the area [6]. Depending on the distribution of land and water, the position of the ITD can shift by as much as 40 to 45 degrees of latitude to the north or south of the equator. In spite of these differences, the ITD correlates rather strongly with the height of the sun and indicates the time of day when the sun is at its highest position in the sky.

Table 1. Geographic coordinate of the study locations

Study Location	Latitude (^{O}N)	Longitude (^{O}E)	Vegetation
Sokoto	13.07	5.23	Short Grass Savannah
Katsina	12.98	7.62	Short Grass Savannah
Kano	12	8.59	Short Grass Savannah
Maiduguri	11.83	13.15	Short Grass Savannah
Ibadan	7.38	3.95	Rain Forest
Ado-Ekiti	7.61	5.24	Rainforest
Ogbomosho	8.12	4.24	Woodland and Tall grass Savannah
Ilorin	8.47	4.54	Woodland and Tall grass Savannah
Osogbo	7.78	4.54	Woodland and Tall grass Savannah
Lagos	6.52	3.37	Fresh Water Swamp
Yenagoa	4.92	6.67	Fresh Water Swamp
Benin	6.33	5.6	Rainforest
Port Harcourt	4.82	7.05	Fresh Water Swamp

Study Location	Latitude (^{O}N)	Longitude (^{O}E)	Vegetation
Warri	5.55	5.79	Rainforest
Minna	9.58	6.54	Rainforest
Jos	9.9	8.86	Woodland and Tall grass Savannah
Abeokuta	7.15	3.36	Rainforest
Bida	9.08	6.01	Woodland and Tall grass Savannah
Abuja	9.07	7.48	Woodland and Tall grass Savannah

2.2 Data

Refractivity and refractivity gradient: The radio refractivity, denoted as (N) is mathematically represented as;

$$\mathrm{N} = 77.6\frac{\mathrm{P}}{\mathrm{T}} + 3.73\mathrm{X}10^{5}\frac{\mathrm{e}}{\mathrm{T}^{2}} \quad \text{(N-units)} \qquad (1.1)$$

Equation (1.1) above is divided into two parts

$$N = N_{DRY} + N_{WET} \qquad (1.2)$$

where,

$$N_{DRY} = 77.6\frac{P}{T}$$

$$N_{WET} = 3.73X10^{5}\frac{e}{T^{2}}$$

where,

- P= atmospheric pressure (hpa),
- e = water vapour pressure (hpa),
- T= absolute temperature (K)

The differential equation that describes the relationship between the water vapour pressure, e (hPa), the saturation vapour pressure, es (hPa), and the relative humidity, H (%), may be derived from equation (1.2) as follows:

$$\mathrm{e} = \frac{\mathrm{H}}{100}\mathrm{es} \qquad (1.3)$$

where,

$$es = a \exp\left[\frac{bt}{t+c}\right] \qquad (1.4)$$

The values of the coefficients in equation (1.4) are obtained as a = 6.1121, b = 17.502, c = 240.97. The atmospheric temperature, denoted as T, is measured in Kelvin (K), whereas the dry atmospheric pressure, represented by P in (hPa). Additionally, the temperature, denoted as t in (°C).

Hence, the Refractivity Gradient in N-units per km may be represented as:

$$G = \frac{\mathrm{dN}}{\mathrm{dh}} = \frac{\mathrm{N_{1km}} - \mathrm{N_s}}{\Delta\mathrm{h}} \qquad (1.5)$$

Where $\mathrm{N_{1km}}$ is the refractivity at 1 km height is, N_s is the refractivity at the surface, Δh is change in height.

The connection between the Latitudinal (L) location of the Intertropical discontinuity (ITD), which is the independent variable, and the Refractivity Gradient (RG), which is the dependent variable, was investigated using five regression models in this work.

2.3 Regression Line. Equations Adopted

a. LINEAR: $L = B_0 + B_1R_G$ (1.6)

where B_0 is the intercept and B_1 is the slope

b. QUADRACTIC: $L = RG^2 + RG + B_0$ (1.7)

c. CUBIC: $L = -RG^3 - RG^2 - RG - B_0$ (1.8)

d. LOG: $LnRG = - B_0 + B_1LnL$ (1.9)

e. POWER**:** $RG = - B_0 + B_1LnL$ (2.0)

3. RESULTS

In order to establish the relationship between Refractivity gradient and Intertropical Discontinuity, a linear and multiple regression model were conducted, with ITD parameters such as; mean daily values of Latitudes, longitudes and dewpoint temperatures were modelled against mean daily values of Refractivity Gradient, however, it was discovered that only the latitudinal positions of the Intertropical Discontinuity were suitable for these models while other parameters like dewpoint temperatures, longitudinal positions were insignificant for both linear and multiple regressions adopted in this work as calculated in the tables shown below across the various regions in Nigeria.

L (latitudinal position of ITD) is the independent variable or predictor in these models while Refractivity Gradient is the dependent variable. The models performed better in the Derived and Guinea savannah regions with about 98%

coefficient of determination followed by Sub-sahelian and Coastal regions with 97% coefficient of determination. All of the predictors explain a large amount of the variance between the variables. R^2 = 0.984-0.973) across all stations; it shows that the variability of L is explained by 97-98% of the variance of RG, the coefficient of multiple correlation (R) = 0.986 explains the strong correlation between the predicted data and the observed data. Overall, it was discovered that cubic regression model has the highest correlation amongst other models.

3.1 Validation of Model (Actual Vs Predicted Values of Refractivity Gradients

3.1.1 Coastal region

The values of the actual refractivity gradients against predicted refractivity gradients are plotted below Fig. 1. Also, the differences in the values obtained becomes smaller as we move down the year from January to December. In this region, R^2 = 0.9862 signifies its ability to find the probability of future events occurring within the given predicted results outcomes. If more samples are added to the model, the coefficient will show the likelihood or the probability of a new point or the new dataset falling on the line.

The correlation coefficient in this region is 0.9862, the correlation is positive. It shows there is a strong linear relationship between Actual RG and Predicted RG. As Actual RG increases, Predicted RG also appears to increase. While R^2 suggests that 97% of changes Actual RG to changes in Predicted RG, 3% are unexplained which justifies that this model can be used to forecast future values of Refractivity gradients provided that the latitudinal position of ITD is known for stations in the coastal region.

3.1.2 Derived region

The values of the actual refractivity gradients against predicted refractivity gradients are plotted below as shown in Fig. 2. Also, the differences in the values obtained becomes smaller as we move down the year from January to December in this region. R^2 = 0.9918 signifies its ability to find the probability of future events occurring within the given predicted results outcomes. If more samples are added to the model, the coefficient will show the likelihood or the probability of a new point or the new dataset falling on the line.

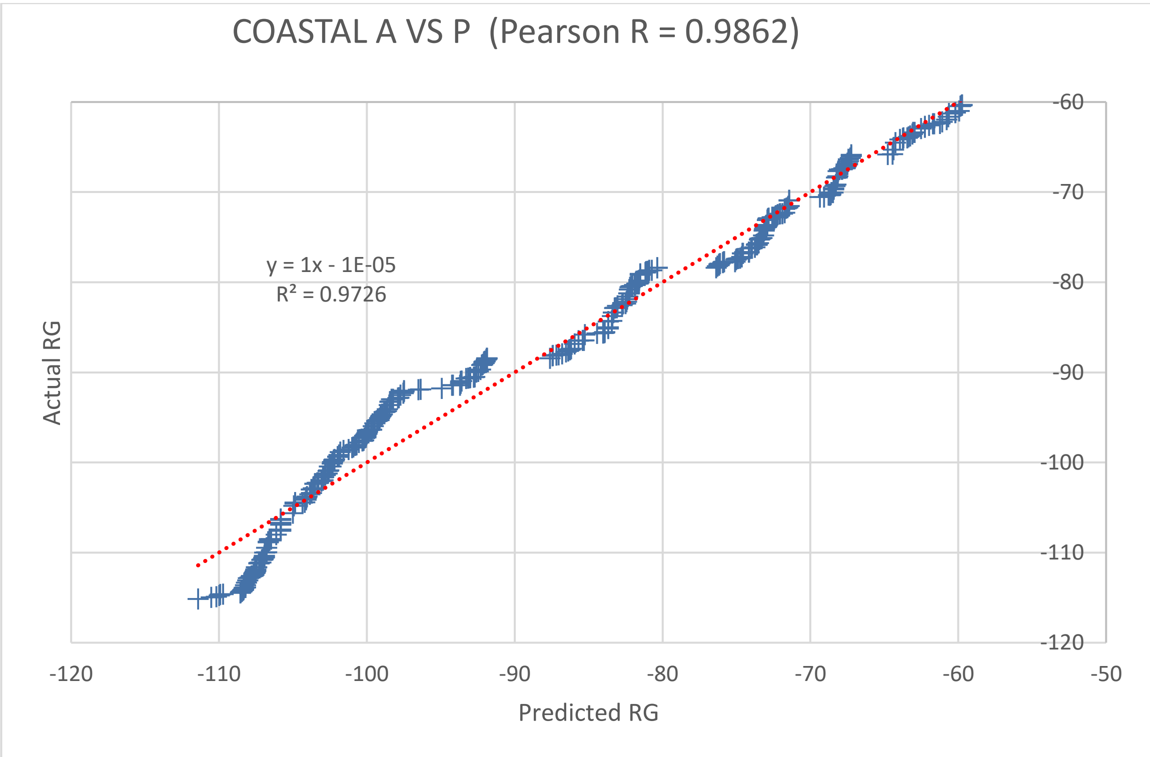

Fig. 1. Actual Vs Predicted Values of Refractivity Gradients (Coastal Region)

Table 2. Models for Coastal Region

Models	N	B_0	SEB_0	B_1	SEB_1	B_2	SEB_2	B3	SEB_3	R	R^2	F	P-value
Linear	365	34.796	6.889	0.252	554e-6	-		-	-	0.972	0.973	12,882	0.0000
Quadratic	365	49.310	43.097	0.591	0.012	0.002	2e-7	-	-	0.992	0.984	11,608	1.72e-181
Cubic	365	-20.915	-76.925	-1.897	-0.245	-0.027	3.78e-5	-109e-4	6.182e-10	0.996	0.992	15,857	3.24e-8
Log	365	-5.824	-0.069	0.549	2.6e-4	-	-	-	-	0.986	0.972	12,837	0.0000
Power	365	-206.193	-170.315	47.611	15.664	-	-	-	-	0.991	0.983	20,856	0.0000

Table 3. Models for Derived Region

Models	N	B_0	SEB_0	B_1	SEB_1	B_2	SEB_2	B3	SEB_3	R	R^2	F	P-value
Linear	365	46.430	11.286	0.6027	259e-5	-		-	-	0.992	0.982	19,582	0.0000
Quadratic	365	64.760	130.038	1.269	0.093	0.006	3.9e-6	-	-	0.994	0.985	12,080	3.13e-18
Cubic	365	-175.029	-2457	-11.833	-9.040	-0.231	0.003	-0.0014	1.12e-7	0.997	0.992	14,699	7.13e-33
Log	365	-4.9135	-0.039	0.3599	115e-5	-	-	-	-	0.915	0.972	12,686	0.0000
Power	365	-105.739	-37.537	19.995	2.839	-	-	-	-	0.994	0.982	19,935	0.0000

Table 4. Models for Guinea Savannah

Regression Models	N	B_0	SEB_0	B_1	SEB_1	B_2	SEB_2	B3	SEB_3	R	R^2	F	P-value
Linear	365	15.130	0.4796	0.1099	813e-7	-	-	-	-	0.992	0.984	22,009	0.0000
Quadratic	365	14.909	0.443	0.1218	125e-6	268e-6	505e-11			0.994	0.989	17,188	1.09e-30
Cubic	365	15.177	0.4356	0.1289	116e-6	-18e-5	-579.6e-12	-7.10E-6	-3.24e-12	0.997	0.994	19,190	5.1e-8
Log	365	-22.558	-11.103	8.497	1.665	-	-	-	-	0.915	0.838	1,872	0.0000
Power	365	-296.249	-463.630	110.129	68.776	-	-	-	-	0.994	0.989	31,100	0.0000

Table 5. Models for Sahel Region

Models	N	B_0	SEB_0	B_1	SEB_1	B_2	SEB_2	B3	SEB_3	R	R^2	F	P-value
Linear	365	11.944	0.334	0.0491	1.62e-5	-	-	-	-	0.991	0.983	20,865	0.0000
Quadratic	365	11.642	0.403	0.048	1.49e-5	4.758E-5	188.6e-12	-	-	0.994	0.988	14,619	0
Cubic	365	11.490	0.299	0.055	27e-6	8.601E-5	306.8e-12	-7.19e-7	-284.87e-16	0.998	0.994	18,695	2.96e-65
Log	365	-29.397	-11.406	12.003	1.858	-	-	-	-	0.971	0.943	6,013	0.0000
Power	365	-596.790	-2381.79	245.932	391.523	-	-	-	-	0.993	0.985	23,853	0.0000

The correlation coefficient in this region is 0.9902, the correlation is positive. It shows there is a strong linear relationship between Actual RG and Predicted RG. As Actual RG increases, Predicted RG also increases. While R^2 suggests that 98% of changes Actual RG to changes in Predicted RG, 2% are unexplained which justifies that this model can be used to forecast future values of Refractivity gradients provided that the latitudinal position of ITD is known for stations in the derived region. This also implies the model is more accurate in the derived region by 1% over the coastal region.

3.1.3 Guinea region

The values of the actual refractivity gradients against predicted refractivity gradients are plotted below and shown. In Fig. 3. The differences in the values obtained becomes smaller as we move down the year from January to December in this region. R^2 = 0.9804 signifies its ability to find the probability of future events occurring within the given predicted results outcomes. If more samples are added to the model, the coefficient will show the likelihood or the probability of a new point or the new dataset falling on the line.

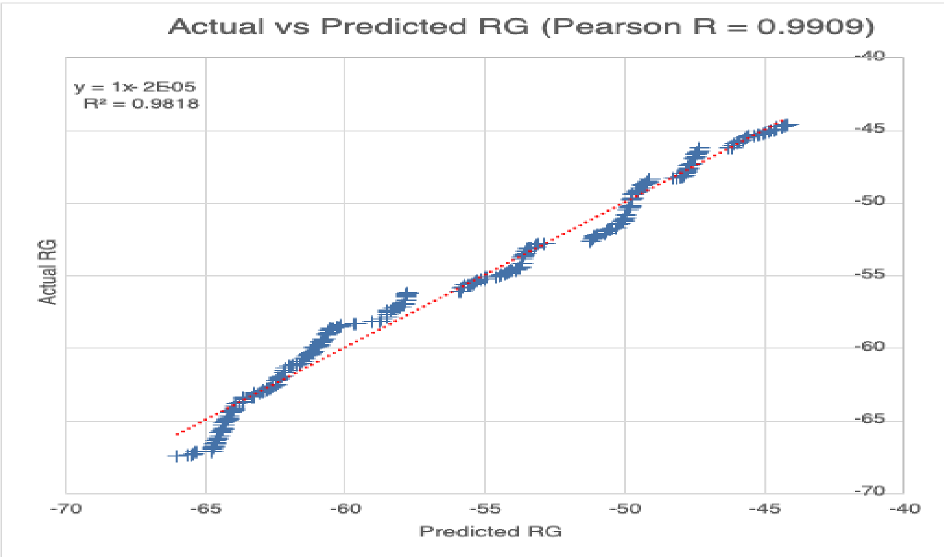

Fig. 2. Actual Vs Predicted Values of Refractivity Gradients (Derived Region)

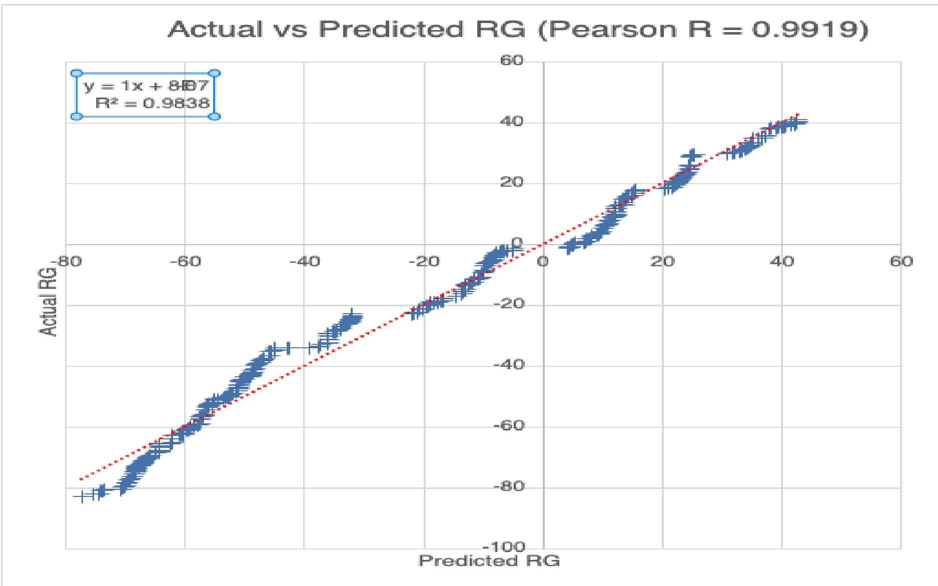

Fig. 3. Actual Vs Predicted Values of Refractivity Gradients (Guinea Region)

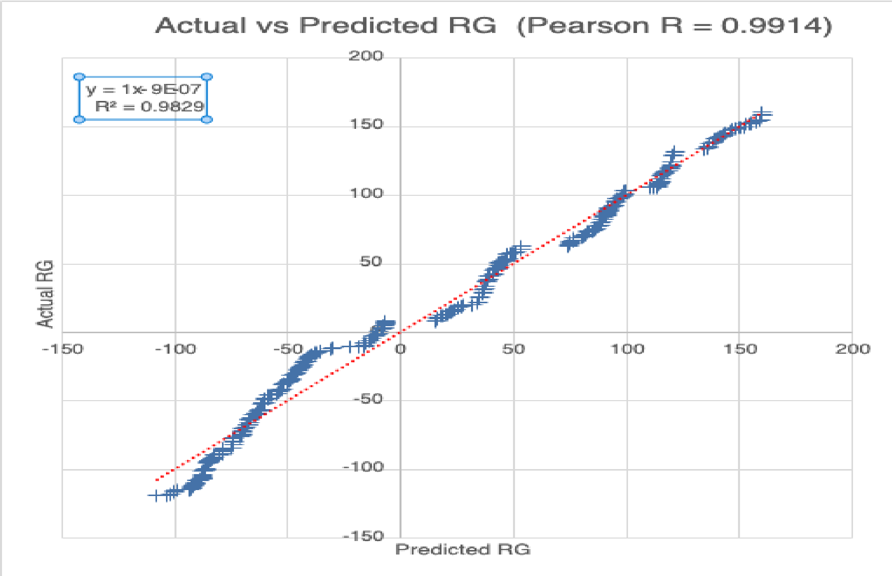

Fig. 4. Actual Vs Predicted Values of Refractivity Gradients (Sub-Sahelian Region)

The correlation coefficient in this region is 0.9919, the correlation is positive. It shows there is a stronger linear relationship between Actual RG and Predicted RG. As Actual RG increases, Predicted RG also increases. While R^2 suggests that 98% of changes Actual RG to changes in Predicted RG, 2% are unexplained which justifies that this model can be used to forecast future values of Refractivity gradients provided that the latitudinal position of ITD is known for stations in the Guinea Savanna region. This also implies the model is more accurate in the Guinea region over the coastal and derived region.

3.1.4 Sub-Sahelian region

The values of the actual refractivity gradients against predicted refractivity gradients are plotted below as shown in Fig. 4. The differences in the values obtained becomes smaller as we move down the year from January to December in this region. $R^2 = 0.9828$ signifies its ability to find the probability of future events occurring within the given predicted results outcomes. If more samples are added to the model, the coefficient will show the likelihood or the probability of a new point or the new dataset falling on the line.

The correlation coefficient in this region is 0.9919, the correlation is positive. It shows there is a stronger linear relationship between Actual RG and Predicted RG. As Actual RG increases, Predicted RG also increases. While R^2 suggests that 98% of changes Actual RG to changes in Predicted RG, 2% are unexplained which justifies that this model can be used to forecast future values of Refractivity gradients provided that the latitudinal position of ITD is known for stations in the Guinea Savanna region. This also implies the model is more accurate in the Sahel region over the coastal and derived region.

4. CONCLUSION AND RECOMMENDATION

4.1 Conclusion

This work has demonstrated the relationship between refractivity gradients and intertropical discontinuity. Relative to other stations, the coastal stations have lower refractivity values due to their proximity to the ocean. Variations in refractivity gradients are found to be large during dry seasons and very low during wet seasons across all stations. Rainfall distribution at all stations has been found to be influenced by the migration of the intertropical discontinuity (ITD) across all sites. The refractivity gradient value decreases throughout the stations as the ITD's latitudinal position rises. Across the four geographical regions of Nigeria, the regression model constructed for this study demonstrated a positive correlation between the values of the refractivity gradient and the latitudinal position of the Intertropical discontinuity. With almost 98% accuracy, the regression models fared better in the Guinea and Sub-Sahelian regions. Overall, cubic regression model performs best across all regions of study. In addition to helping radio engineers prepare for anomalous propagations in communication fields, this would also aid in the estimation of refractivity gradients for sites with climates comparable to the regions this work is studying.

DISCLAIMER (ARTIFICIAL INTELLIGENCE)

I hereby declare that NO generative AI technologies such as Large Language Models (ChatGPT, COPILOT, etc) and text-to-image generators have been used during writing or editing of manuscripts.

COMPETING INTERESTS

Authors have declared that no competing interests exist.

REFERENCES

1. Dairo OF, Kolawole LB. Radio refractivity gradients in the lowest 100m of the atmosphere over Lagos, Nigeria in the rainy-harmattan transition phase. Journal of Atmospheric and Solar-Terrestrial Physics. 2018;167:169-76.
2. Emmanuel I, Ojo OS, Abe OE, Adedayo KD. Geostatistical distribution of vertical refractivity gradient over Nigeria. Radio Science. 2020;55(9):1-8.
3. Tanko MM, Sarki MU, Bilya MA. Seasonal Variation of Radio Refractivity of Some Selected Stations in Northern Nigeria. Current Journal of Applied Science and Technology. 2019;32(1):1–12. Available:https://doi.org/10.9734/CJAST/2019/45326
4. Adediji AT, Ajewole M. Vertical Profile of Radio Refractivity Gradient in Akure South-West Nigeria. Progress In Electromagnetics Research C. 2008;4:157-168
5. Arowolo AV, Oluleye A. Assessing the influence of intertropical discontinuity on total column ozone variation over West Africa. Environmental Science and Pollution Research. 2022;29(44):66689-704.
6. Pospichal B, Karam D, Crewell S, Flamant C, Hünerbein A, Bock O, Saïd F. Diurnal cycle of the intertropical discontinuity over West Africa analysed by remote sensing and mesoscale modelling. Quarterly Journal of the Royal Meteorological Society. 2010;136(S1):92-106.
7. Adejuwon JO, Odekunle TO. Variability and the Severity of the “little Dry Season” in southwestern Nigeria. Journal of climate. 2006;19(3):483-93.
8. Adeyemi B, Aro TO. Variation in surface water vapour density over four Nigerian stations. Nigeria Journal of Pure and Applied Physics. 2004;3.
9. Adeyemi B. Surface water vapour density and tropospheric radio refractivity linkage over three stations in Nigeria. Journal of Atmospheric and Solar-Terrestrial Physics. 2006;68(10):1105-15.
10. Ayanlade A, Atai G, Jegede MO. Spatial and seasonal variations in atmospheric aerosols over Nigeria: assessment of influence of intertropical discontinuity movement. Journal of Ocean and Climate. 2019;9:1759313118820306.
11. Balin I. Measurement and analysis of aerosols, cirrus-contrails, water vapor and temperature in the upper troposphere with the Jungfraujoch LIDAR system. EPFL; 2004.
12. Akpootu DO, Rabiu AM. Empirical Models for Estimating Tropospheric Radio Refractivity Over Osogbo, Nigeria. The Open Atmospheric Science Journal. 2019; 13(1).
13. Bettouche Y, Agba B, Kouki AB, Obeidat H, Alabdullah A, Abdussalam F, Ghauri S, Abd-Alhameed RA. Estimation and analysis of the radio refractivity, its gradient and the geoclimatic factor in Arctic regions. Progress In Electromagnetics Research M. 2020;92:181-92.
14. Dairo OF, Kolawole LB. Statistical analysis of radio refractivity gradient of the rainy-harmattan transition phase of the lowest 100 m over Lagos, Nigeria. J. Atmos. Sol.-Terr. Phys; 2017.
15. Ojo JS, Adelakun AO, Edward OV. Comparative study on radio refractivity gradient in the troposphere using chaotic quantifiers. Heliyon. 2019;5(8).
16. Fashade OO, Omotosho TV, Akinwumi SA, Olorunyomi KP. Refractivity gradient of the first 1km of the troposphere for some selected stations in six geo-political zones in Nigeria. InIOP Conference Series: Materials Science and Engineering. 2019;640(1):012087).
17. Benzon H, H∅eg P, Wave propagation simulation of radio occultations based on ECMWF refractivity profiles, in Radio Science. 2015;50(8):778-788. DOI: 10.1002/2015RS005649.
18. Emmanuel I, Adeyemi B, Ogolo EO, Adediji AT. Characteristics of the

anomalous refractive conditions in Nigeria. Journal of Atmospheric and Solar-Terrestrial Physics. 2017;164:215-21.
19. Ogunsua BO, Ojo JS, Adediji AT. Atmospheric chaoticity and complexity from radio refractivity derived from Akure station. Advances in Space Research. 2018;62(7):1690-701.
20. Lawal YB, Omotoso ET. Investigation of Point Refractivity Gradient and Geoclimatic Factor at 70 m Altitude in Yenagoa, Nigeria. Journal of the Nigerian Society of Physical Sciences. 2023:1081.
21. Diallo I, Bain CL, Gaye AT, Moufouma-Okia W, Niang C, Dieng MD, Graham R. Simulation of the West African monsoon onset using the HadGEM3-RA regional climate model. Climate dynamics. 2014; 43:575-94.
22. Willoughby AA, Aro TO, Owolabi IE. Seasonal variations of radio refractivity gradients in Nigeria. Journal of Atmospheric and Solar-Terrestrial Physics. 2002;64(4):417-25.
23. Pospichal B, Karam D, Crewell S, Flamant C, Hünerbein A, Bock, O, Saïd F. Diurnal cycle of the intertropical discontinuity over West Africa analysed by remote sensing and mesoscale modelling. Quarterly Journal of the Royal Meteorological Society. 2010;136(S1):92-106.
Available:https://doi.org/10.1002/qj.435
24. Schneider T, Bischoff T, Haug GH. Migrations and dynamics of the intertropical convergence zone. Nature. 2014;513(7516):45-53.
25. Zhang T, Tan G, Bai W, Sun Y, Wang Y, Luo X, Song H, Sun S. A Disturbance Frequency Index in Earthquake Forecast Using Radio Occultation Data. Remote Sensing. 2023; 15(12):3089.

Peer-review history:
The peer review history for this paper can be accessed here:
https://doi.org/10.9734/ajarr/2024/v18i11788118040